Electronic Supplementary Material (ESI) for Dalton Transactions.

Deposition of Tetraferrocenylporphyrins on ITO surface for photo-catalytic O_2 activation

F. Sabuzi,[†] M. Tiravia,[†] A. Vecchi, E. Gatto, M. Venanzi, B. Floris, V. Conte [*] and P. Galloni [*]

Dipartimento di Scienze e Tecnologie Chimiche, Università di Roma Tor Vergata, Via della Ricerca Scientifica, 00133 Rome, Italy

Index

Products characterization

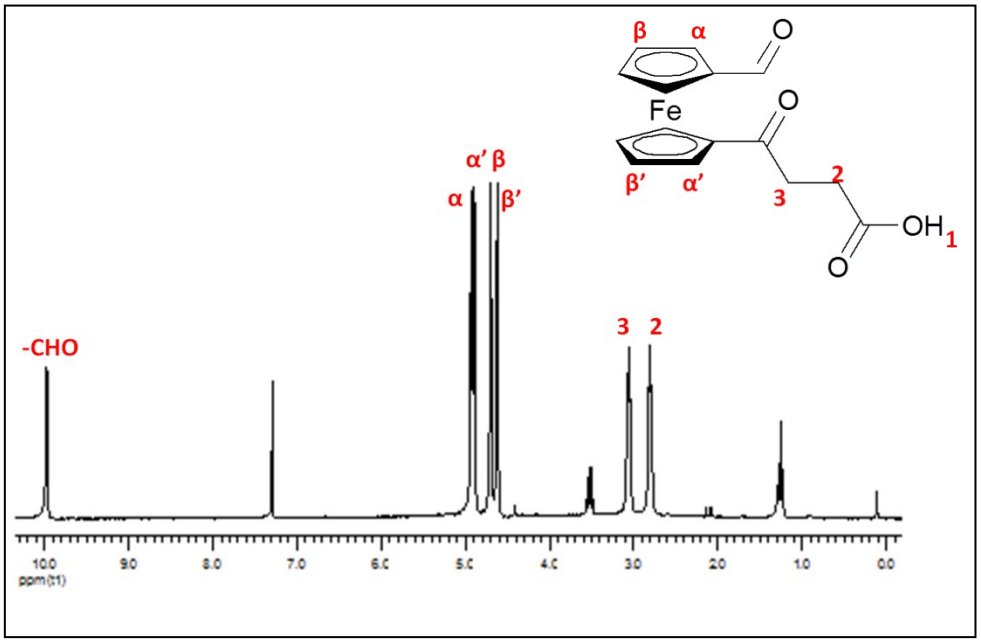

Figure S1. ^{1}H NMR spectrum of 4-(1'-formyl)ferrocenyl-4-oxobutanoic acid (**1**) in $CDCl_3$.

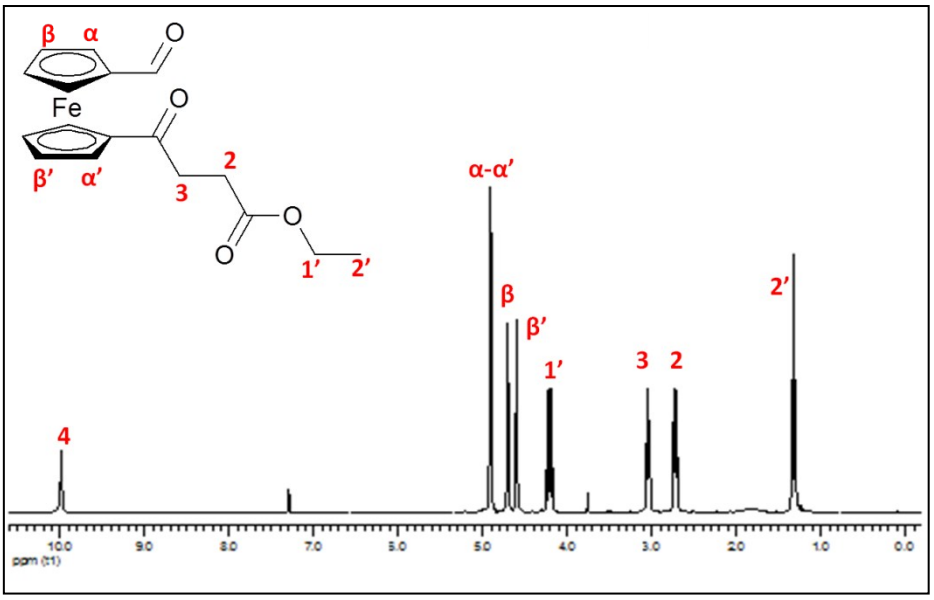

Figure S2. ^{1}H NMR spectrum of ethyl 4-(1'-formyl)ferrocenyl-4-oxobutanoate (**2**) in $CDCl_3$.

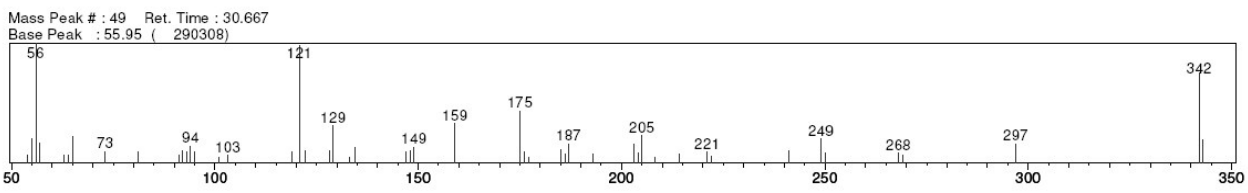

Figure S3. MS (ESI) of ethyl 4-(1'-formyl)ferrocenyl-4-oxobutanoate (**2**).

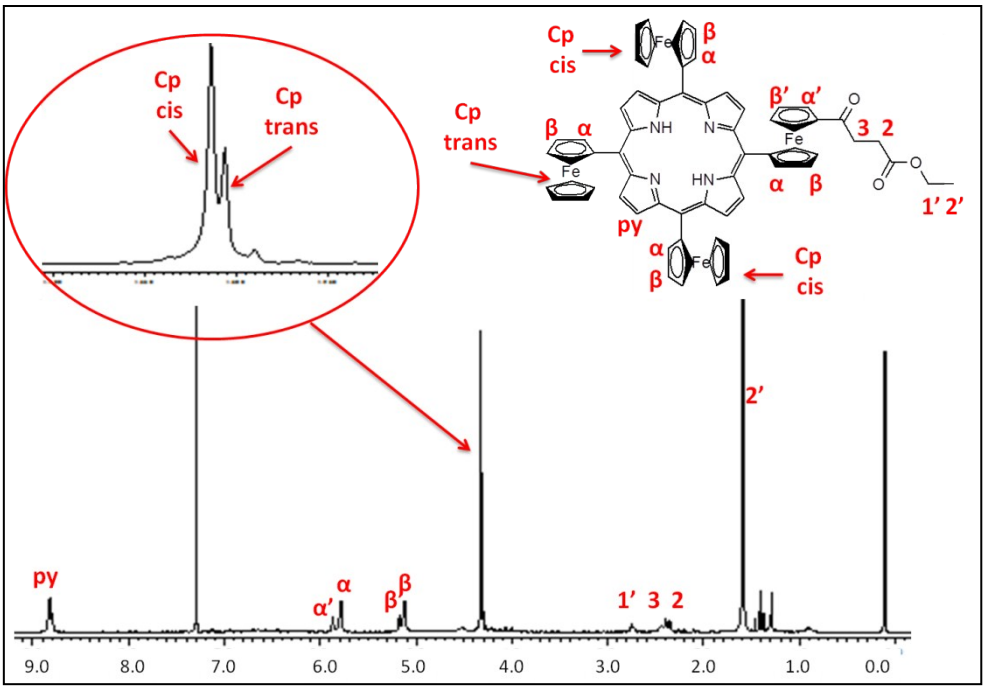

Figure S4. ^{1}H NMR of 5-[1'-(3-ethoxycarbonyl-1-oxopropyl)ferrocenyl]-10,15,20-triferrocenylporphyrin (**3**) in $CDCl_3$.

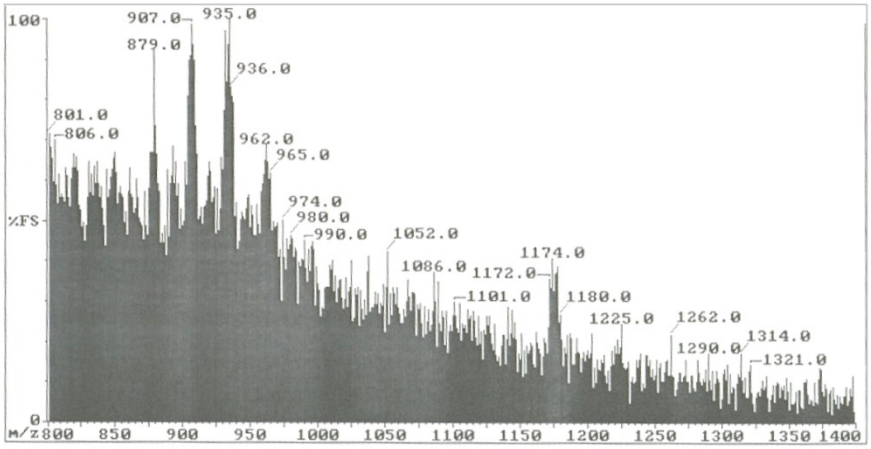

Figure S5. MS (FAB) of 5-[1'-(3-ethoxycarbonyl-1-oxopropyl)ferrocenyl]-10,15,20-triferrocenylporphyrin (**3**) using 3-nitrobenzyl alcohol matrix.

Surface pressure - mean molecular area isotherm of porphyrin 4

To construct the isothermal curve, 100 µl of a 0.2 mg/ml solution of porphyrin **4** in $CHCl_3$ have been spread on the Milli-Q water subphase. Following solvent evaporation, the gradual compression of the film has been performed at the rate of 5 mm/min and at constant temperature of 25°C. Isothermal curve is reported in Fig. S6.

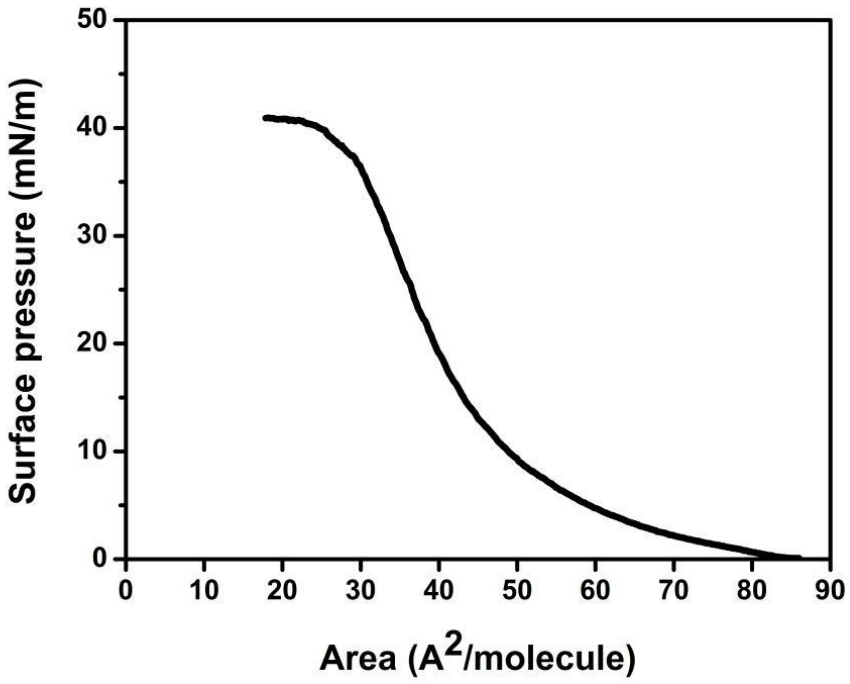

Figure S6. Surface pressure - mean molecular area isotherm of porphyrin **4**.

Surface pressure - mean molecular area isotherm of H_2TFcP

150 µl of a 0.2 mg/ml solution of H_2TFcP in $CHCl_3$ have been spread on the Milli-Q water subphase. The solvent was allowed to evaporate for 30 minutes, at constant temperature (25°C).

Compression of the film has been performed at the rate of 5 mm/min. A gradual increase in the surface pressure was observed.

At surface pressure values higher than 45 mN/m the phase transition takes place. To ensure the preparation of homogeneous mono- and multilayers, depositions have been carried out at a surface pressure of 30 mN/m. Isothermal curve is reported in Fig. S7.

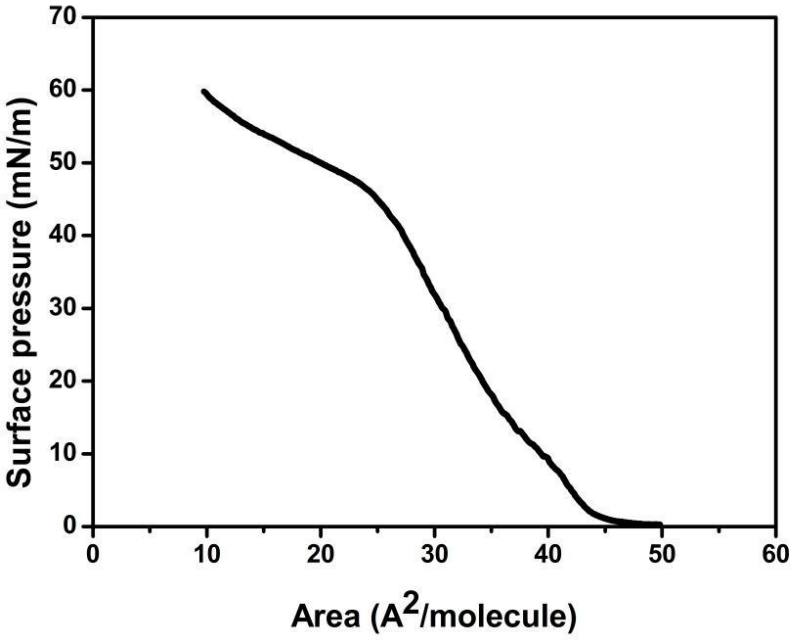

Figure S7. Surface pressure - mean molecular area isotherm of H_2TFcP.

ITO contribution in photocurrent generation

To evaluate ITO contribution in photocurrent generation measurements, a blank experiment has been carried out, using non-functionalized ITO as working electrode, a platinum counter electrode and an Ag/AgCl (sat. KCl) reference electrode. Measurements have been performed in an aqueous solution of 0.1 M Na_2SO_4. Negligible signals have been detected above 350 nm.

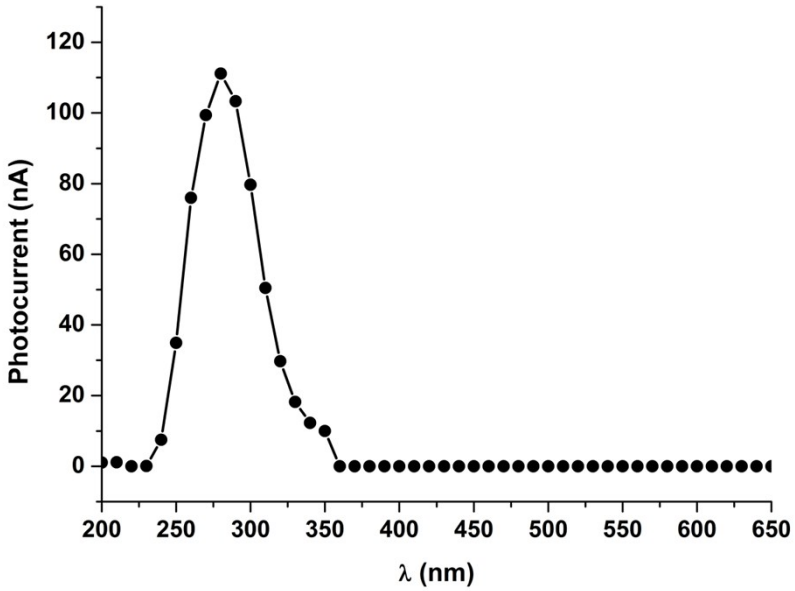

Figure S8. Action spectrum of non-functionalized ITO in H_2O/0.1 MNa_2SO_4 /50 mM TEOA. Applied potential: 0.0 V, *vs*. Ag/AgCl.

UV-vis absorption spectrum of SAM 2 and SAM 3

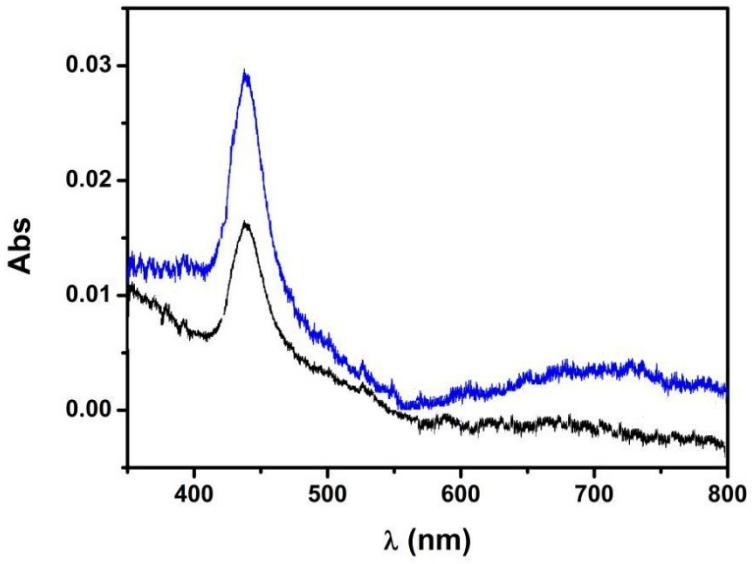

Figure S9. UV-vis absorption spectrum of **SAM 2** (black line) and **SAM 3** (blue line).

Photocurrent generation SAM 1 and SAM 3

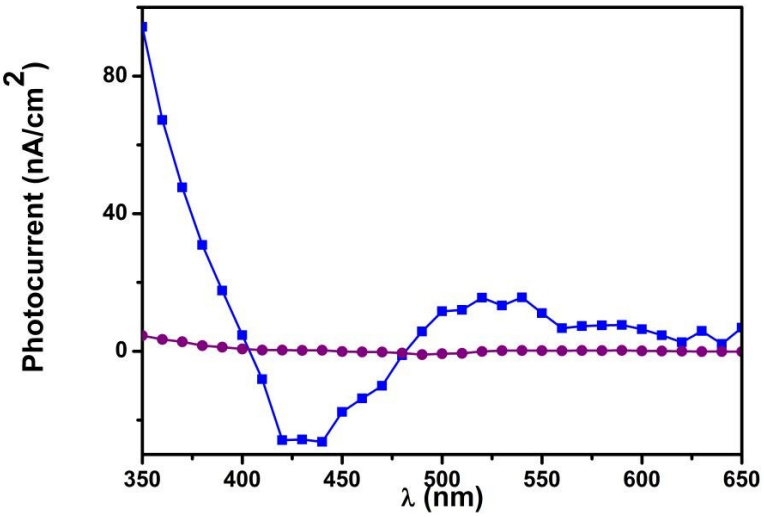

Figure S10. Action spectrum of **SAM 1** (purple line) and **SAM 3** (blue line) in H_2O/0.1 M Na_2SO_4. Applied potential: 0.0 V, *vs*. Ag/AgCl.

SAM 4: characterization and photocurrent

UV-vis absorption spectrum of **SAM 4** (Fig. S11) showed a very intense band between 350 and 550 nm. The absorption spectrum was not well resolved: it was not centered at the Soret band position of compound **4** in solution and, although the higher absorption of **SAM 4** with respect to **SAMs 1** and **3**, the Q-bands were not detectable. Furthermore, the broadness of the Soret band indicates the presence of aggregates on the electrode surface (from interactions either with free or linked porphyrins).

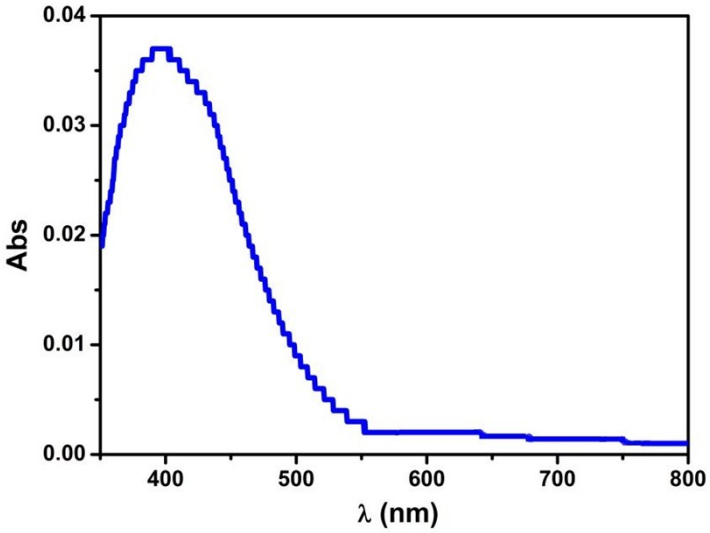

Figure S11. Uv-vis absorption spectrum of **SAM 4**.

Since the absorption spectrum of **SAM 4** was very different from the absorption spectrum of the mono-substituted tetraferrocenylporphyrin (**4**) in solution, to estimate the density of porphyrin molecules bound on the electrode surface, cyclic voltammetry measurements have been carried out, in CH_2Cl_2, using tetrabutylammonium perchlorate (TBAP) 100 mM as supporting electrolyte (Fig. S12). In this experiment it was not possible to detect separately each single process, probably due to aggregation on the electrode surface, thus a reversible four electron process, characterized by a broad signal, has been observed ($E_{½}$=0.5 V). The broadness of the peak constitutes a confirmation of the presence of aggregates on the elctrode surface. However, the monolayer showed great stability, keeping its electrochemical signal constant over many consecutive scans. From the integration of the electrochemical signal it was possible to estimate the surface coverage[1] (Γ=4.9 $\cdot 10^{14}$ molecules$\cdot$cm^{-2}) which was significantly higher than that of **SAMs 1-3**, confirming the high density of **SAM 4**.

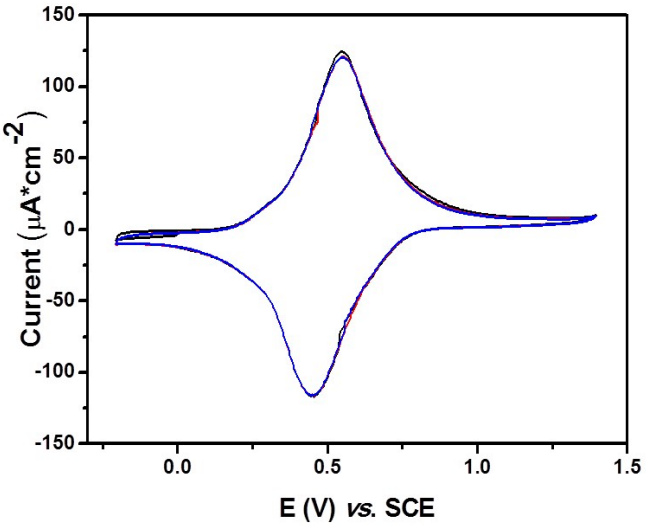

Figure S12. CV of **SAM 4** in CH_2Cl_2/TBAP 100 mM, *vs*. SCE; scan rate 100 mV$\cdot$s^{-1} ((black line: scan 1; red line: scan 2; blue line: scan 3).

SAM 4 has been used as working electrode in photocurrent generation measurements: irradiation of the functionalized-ITO at different wavelengths instantly implied the generation of cathodic photocurrent.

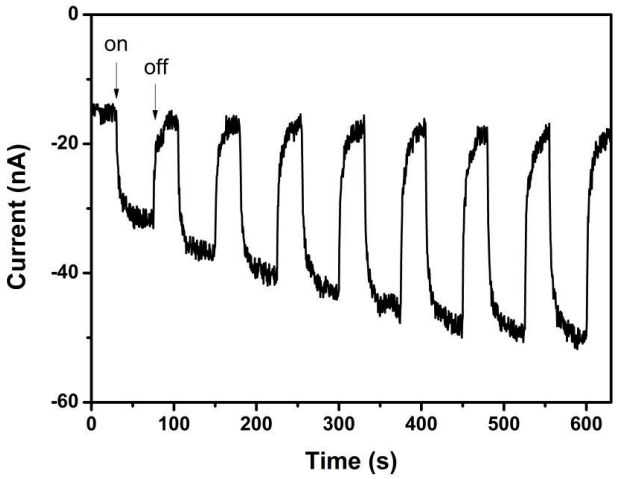

Figure S13. Photoelectrochemical response of ITO/**SAM 4** in H_2O/0.1 M Na_2SO_4, at -0.2 V *vs*. Ag/AgCl, upon irradiation at different wavelengths (from 480 nm to 410 nm every 10 nm) at room temperature; 45 seconds of irradiation were alternated with 30 seconds of dark.

The action spectrum (Fig. S14) was in good agreement with the absorption spectrum of the modified electrode, indicating that the substituted porphyrin acted as the photoactive centre for photocurrent generation. Moreover, the photocurrent increased at lower applied potential at the electrode, where the process is energetically favored. However, the shapes of absorption and action spectra were not well resolved and they did not match with the absorption spectrum of the porphyrin in solution.

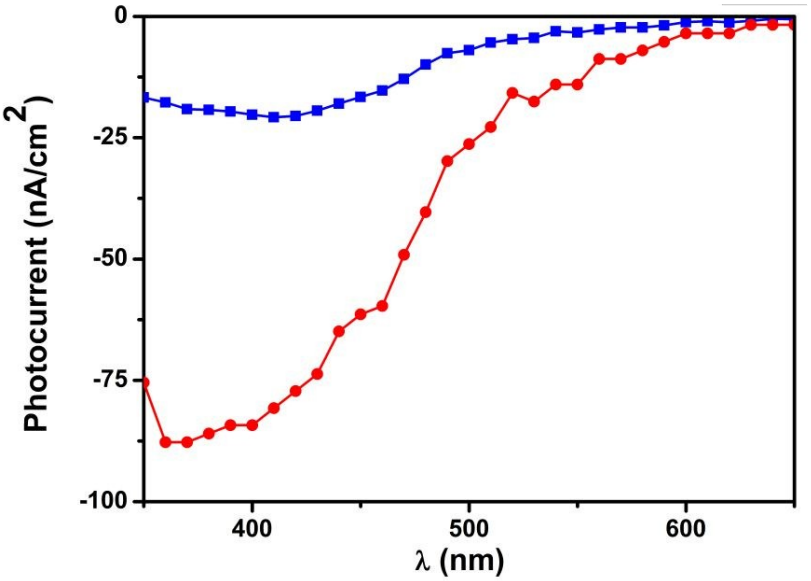

Figure S14. Action spectrum of ITO/**SAM 4** in H_2O/0.1 M Na_2SO_4, at 0.0 V (blue line) and -0.2 V (red line) *vs*. Ag/AgCl.

LB 1-4: stability and photocurrent

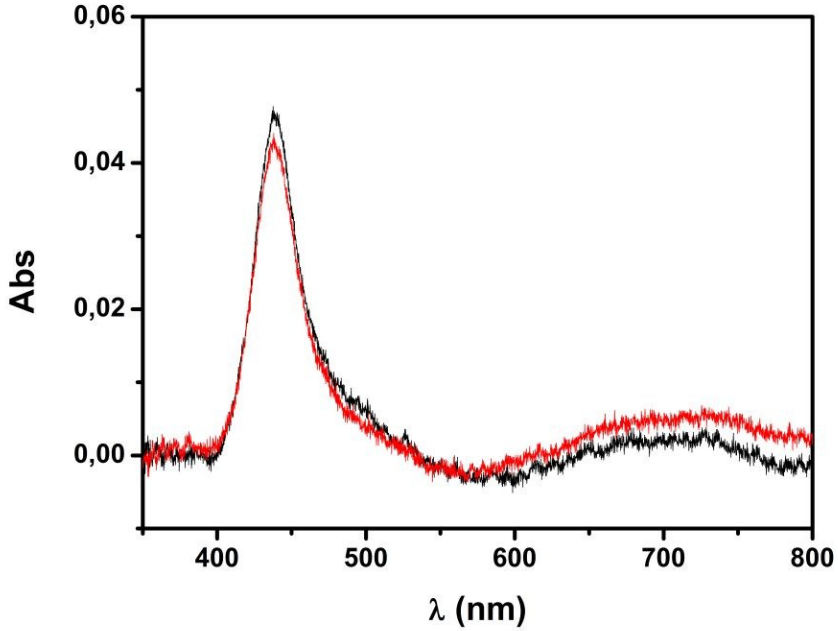

Figure S15. UV-vis spectra of **LB 1** before (black line) and after (red line) photocurrent generation measurements.

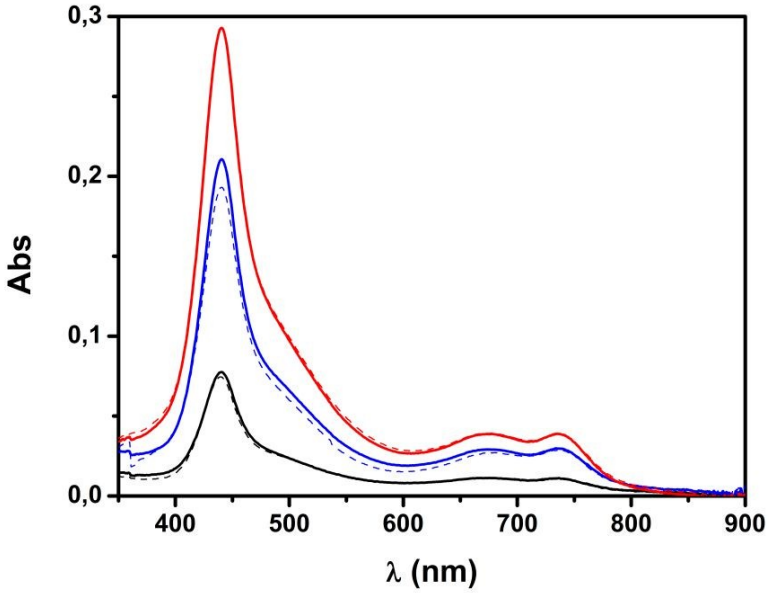

Figure S16. UV-vis spectrum of **LB 2** (one layer, black line), **LB 3** (three layers, blue line) and **LB 4** (five layers, red line) before (solid lines) and after (dashed lines) photocurrent generation measurements.

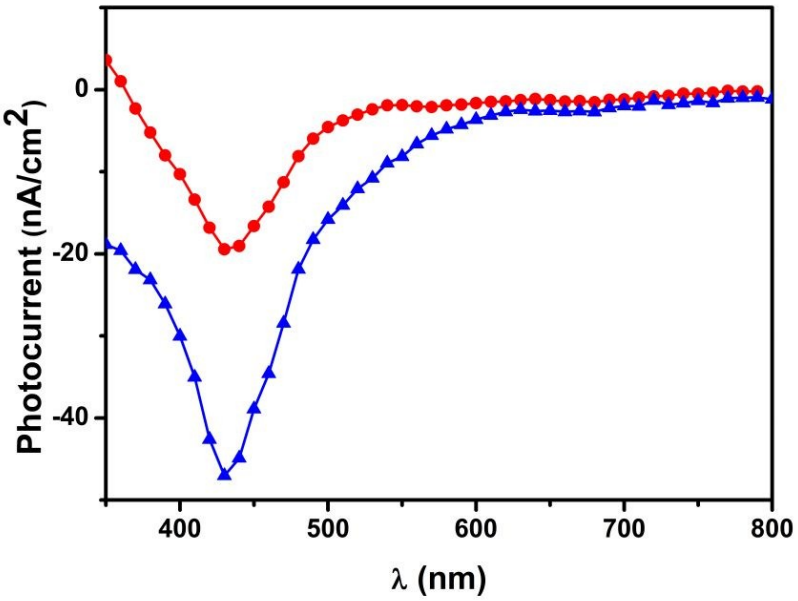

Figure S17. Action spectrum of ITO/**LB 1** in H_2O/0.1 M Na_2SO_4, at 0.0 V (red line) and -0.2 V (blue line) *vs*. Ag/AgCl.

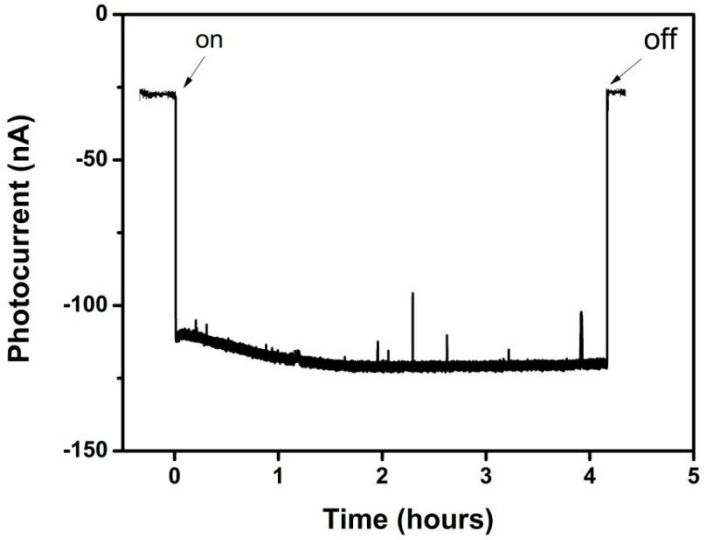

Figure S18. Cathodic photocurrent generation upon excitation at 440 nm, applied potential: -0.2 V *vs*. Ag/AgCl in H_2O/0.1 M Na_2SO_4.

References and notes

1. G. Filippini, Y. Israeli, F. Goujon, B. Limoges, C. Bonal, P. Malfreyt, *J. Phys. Chem. B,* 2011, **115**, 11678. The integration of the oxidative peak on the graph gives the density of the redox-active molecules or surface coverage (Γ) on the electrode through the equation: $\Gamma\ (molecules \cdot cm^{-2}) = Q \cdot (n \cdot F \cdot A)^{-1}$, where Q is the quantity of charge in Coulomb calculated by the integral, n is the number of the electrons exchanged during the redox process (n = 4 for tetraferrocenyporphyrins), F is the Faraday constant ($F = 96485\ C \cdot mol^{-1}$) and A is the immersed area of the electrode (that is calculated twice since both the faces of the electrode contribute to the signal).